ChemPubSoc Europe

DOI: 10.1002/slct.201701960

Chemistry SELECT Communications

Biological Chemistry & Chemical Biology

Versatile Click-Protein Hydrogels for Biomedical Applications

Gunhye Lee,[a, c] Manish Jaiswal,[b] Akhilesh K. Gaharwar,[b] and Zhilei Chen*[c]

Protein hydrogels made entirely of host proteins should be of great value to the field of regenerative medicine. A versatile and efficient approach to transform any protein into hydrogels is presented. This strategy is based on the copper-free click chemistry reaction between azide (N_3) and dibenzylcyclooctyne (DBCO). The target proteins are first individually functionalized with N_3 or DBCO, and then mixed under physiological condition to trigger the spontaneous formation of a highly crosslinked protein network or hydrogel through the click reaction. The resulting click hydrogels exhibited high solution stability, interconnected porous network, tunable compressive moduli ranging from 2 to 200 kPa, adjustable stress-relaxation time ($t_{1/2}$) between 5 and 2200 s, shape-memory property, self-healing ability and the ability to support mammalian cells attachment on 2D and 3D microenvironment, pointing to their great potential in tissue engineering for diverse biomedical applications.

The ability of protein hydrogels to mimic extracellular matrices makes them attractive synthetic materials for regenerative medicine and tissue engineering. Several strategies have been exploited to create protein-based hydrogels in the past two decades.[1] Depending on the crosslinking chemistry, protein hydrogels can be broadly categorized into either physical or chemical hydrogels. Most physically cross-linked protein hydrogels rely on protein-protein/ligand interactions to drive hydrogel formation, such as hydrophobic interactions between coiled-coil synthetic proteins,[2] resilin-like polypeptides,[3] gelatin[4] and collagen,[5] and specific protein-ligand interactions between heparin and heparin-binding growth factor (VGEF),[6] repeats of WW and proline-rich peptide domains,[7] and PDZ and its peptide ligand.[8] Some physical protein hydrogels suffer from poor solution stability due to the reversible nature of the physical interaction.[2b,9] In addition, the proteins that contribute to the specific protein-protein/ligand interactions often derive from artificial or animal sources and, if used as tissue implants, may elicit undesirable foreign body immune responses which can result in inflammation, scaring and even tissue rejection. An ideal protein hydrogel for tissue engineering and regenerative medicine should be composed entirely of host proteins and exhibit tunable mechanical properties to facilitate cell attachment and growth.

Traditional chemical hydrogels are formed using covalent chemical crosslinking agents, such as glutaraldehyde and methacrylic anhydride,[10] which are often cytotoxic. Recently, several enzymes have been explored to generate covalent bonds between different proteins for the synthesis of protein hydrogels with very high cell compatibility, including SpyTag-SpyCatcher,[11] split intein[12] and horse-radish peroxidase.[13] However, these enzymes are all derived from animal or plant sources and are non-ideal for use in the creation of implantable tissue engineering scaffolds. Click chemistry has also emerged as a promising strategy to prepare protein hydrogels due to its high reactivity, superb selectivity, and mild reaction conditions. The photoclick reaction between norbornene and thiol was recently used to form covalently crosslinked gelatin hydrogels.[14] Unfortunately, this thiol-ene crosslinking strategy produces harmful radical species and could cross-react with thiols on cell surface proteins, potentially causing undesirable cytotoxicity. In addition, the photopolymerization reaction requires the input of ultraviolet light (UV), which is toxic to the cells, limiting the clinical translation of the photoclick reaction to settings where rapid UV illumination is possible.[15] The inverse electron demand Diels-Alder click reaction between tetrazine and norbornene has emerged as another popular click chemistry for protein hydrogel formation.[16] However, this reaction releases the nitrogen gas as a side product. Although nitrogen *per se* is harmless in biological systems, the presence of nitrogen bubbles within the resultant hydrogel inevitably affects the hydrogel mechanical integrity during swelling and compression/stretching. The copper-free strain-promoted azide-alkyne cycloaddition (SPAAC) click reaction provides another convenient chemistry for promoting hydrogel formation. Anseth *et al.* successfully utilized the SPAAC reaction to produce hydrogels from the 4-armed PEG tetrazide and an

[a] *G. Lee*
Department of Chemical Engineering
Texas A&M University
College Station, TX, USA
[b] *Dr. M. Jaiswal, Prof. A. K. Gaharwar*
Department of Biomedical Engineering
Texas A&M University
College Station, TX, USA
[c] *G. Lee, Prof. Z. Chen*
Department of Microbial Pathogenesis and Immunology
Texas A&M University
College Station, TX, USA
and
School of Public Health
TAMU 1114
Building 234 A, College Station, TX 77843, USA
Telephone: 979–436-9404
E-mail: zchen4@tamu.edu

Supporting information for this article is available on the WWW under https://doi.org/10.1002/slct.201701960

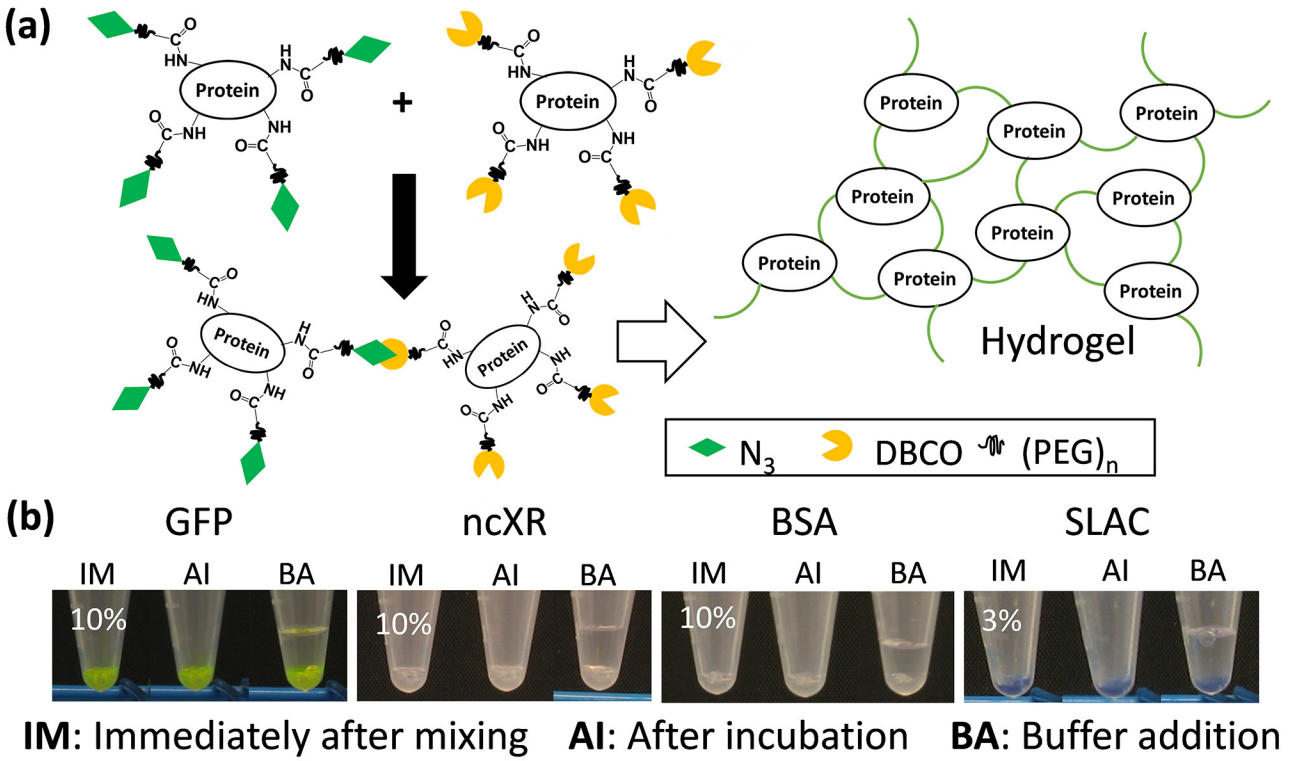

Figure 1. Click protein hydrogel. (a) Schematic of click chemistry reaction between N_3 and DBCO functionalized proteins that triggers the formation of a covalent protein hydrogel. (b) Click protein hydrogels made from different proteins.

Table 1. Model proteins used in the study.

Protein name	Quaternary structure	Monomer Size (kDa)	Protein Unit Size (kDa)	Protein conc (mg/mL)	Molar ratio of protein : N3	Molar ratio of protein: DBCO
GFP	Monomer	29.4	29.4	10	1:8	1:12
ncXR	Dimer	38.5	77.0	20	1:8	1:16
BSA	Weak dimer	66.5	133	20	1:14	1:14
SLAC	Trimer	38.4	115.2	10	1:8	1:8

GFP: green fluorescent protein; ncXR: xylose reductase from *Neurospora crassa*;[22] BSA: bovine serum albumin; SLAC: small laccase from *Streptomyces coelicolor*.[23] The quaternary structure and the molecular weight for each protein were predicted based on the protein's crystal structure and primary amino acid sequence, respectively.

alkene-functionalized peptides.[17] In another study, Song *et al.* reported a biodegradable hydrogel formed through SPAAC under physiological conditions from the azide-containing PEG_co-poly(5,5-bis(azidomethyl)-1,3-dioxan-2-one) and dibenzocyclooctyne (DBCO)-functionalized PEG.[18] Similar polymer-synthetic peptide hybrid hydrogels have been developed using the SPAAC chemistry,[19] and these have found applications ranging from cell encapsulation[20] to drug release.[21] However, so far, SPAAC has so not been used for the creation of hydrogels from globular proteins.

In the current work, we developed a SPAAC-mediated protein ligation approach that enables the creation of hydrogels from essentially any protein, making it possible to produce hydrogels composed entirely of host proteins. The overall scheme for click-protein hydrogel formation is outlined in Figure 1a. To form a crosslinked protein network or hydrogel, each hydrogel building block protein unit needs to be labeled with at least three functional groups. We define protein unit (PU) as the smallest unit of protein(s) that can form a hydrogel crosslink. Each protein unit consists of one protein molecule for monomeric proteins or two protein molecules for dimeric proteins. The hydrogel building block proteins were first functionalized with N_3-PEG_4 or DBCO-PEG_5 *via* primary amine-NHS ester reaction as described in the materials and methods. The reaction pH, incubation time and the ratio of protein to each chemical were tuned in order to preserve protein solubility and ensure that there are at least 3 functional groups on each protein unit. Four model proteins of different sizes and quaternary structures were labeled with the N_3- and DBCO-functional groups. The exact functionalization condition for each protein can be found in Table 1.

The extent of protein functionalization is semi-quantitatively evaluated *via* visualization on SDS-PAGE gel after reaction with dye molecules carrying the respective opposite functional group (Figure S1).[24] As a preliminary evaluation of the hydrogel formation, N_3- and DBCO-functionalized proteins were mixed at 1:1 molar ratio in microcentrifuge tubes (20 μL total) and incubated at room temperature. The next day, PBS (100 μL) was added to each tube. A clear interface between the protein and the PBS solution indicates the formation of a hydrogel (Figure 1b). According to this method, all model proteins were able to form click protein hydrogels, although the minimum protein concentration needed for hydrogel formation varies (Figure S2). In general, higher number of functional groups per PU leads to more stable protein hydrogels.

The 3D structure and the surface topography of click protein hydrogels were analyzed using scanning electron microscopy (SEM). As shown in Figure 2a, click hydrogels

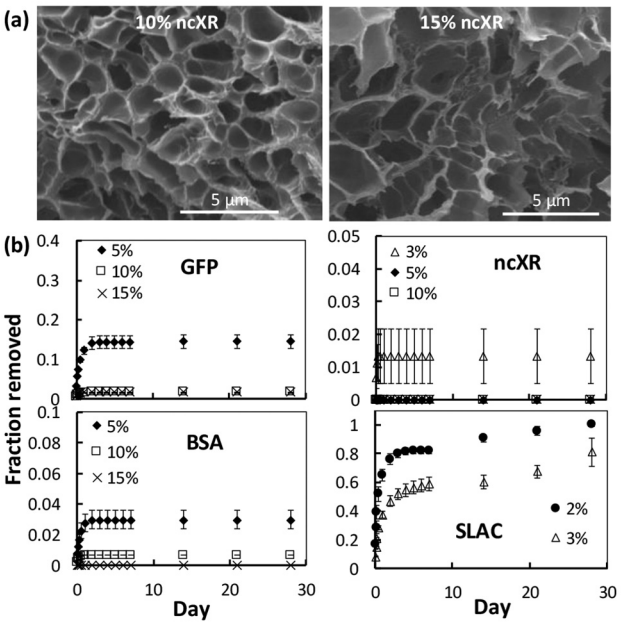

Figure 2. (a) SEM images of 3D microstructure of ncXR hydrogels. (b) Erosion profile of protein hydrogels in PBS for 4 weeks at room temperature.

appeared as smooth sheets-like entangled microstructures that form a highly porous 3D network with pore diameters ranging between 1 and 3 μm. We next evaluated the solution stability of our click protein hydrogels. Cured click protein hydrogels composed of different concentrations of the various building block proteins were immersed in erosion buffer for 28 days at room temperature. The erosion buffer was replaced periodically and the amount of protein in the buffer was quantified using the BCA assay (Figure 2b). Overall, click protein hydrogels exhibited high solution stability. At 5% w/v protein concentration, the hydrogel made of monomeric GFP eroded ~15%, while those made of dimeric ncXR and BSA eroded <4%. Negligible amount of protein erosion (<1%) was observed for GFP, ncXR and BSA click hydrogel at protein concentration equal or above 10% w/v. On the other hand, the trimeric SLAC hydrogel were not stable during prolonged incubation in erosion buffer, likely due to the low protein concentration and/or the low functionalization efficiency and/or dissociation of the trimeric SLAC. Efforts to increase the labeling efficiency of SLAC, as well as to increase the concentration of SLAC in a click protein hydrogel, were not successful due to severe precipitation of this protein under these conditions. Our results confirmed that click protein hydrogels of high solution stability can be easily produced. Furthermore, the erosion profile of these click protein hydrogels can be tuned by adjusting the concentration and/or the labeling efficiency of the hydrogel building block proteins.

The mechanical stiffness of click protein hydrogels made of different proteins were evaluated using the uniaxial compression test. The rates of compressive stress increased with strain for all hydrogels (Figure 3a, Figure S3a, b), indicating that these hydrogels can be easily deformed under low strain but exhibit strong stiffness at high strain. This hydrogel behavior is similar to that of human soft tissues such as collagen[25] and elastin.[26] The hydrogel peak stress (at 0.5 mm/mm strain) varied between 8.6 - 280 kPa (Figure 3b). Not surprisingly, higher density of functional groups on each protein unit and higher protein concentration lead to higher peak stress. The hydrogel compressive modulus, calculated from the initial linear region (0.05-0.2 mm/mm strain), follows a similar trend as the peak stress and varies broadly between 5 to 200 kPa for the different hydrogels (Figure 3d). These peak stress and compressive modulus are comparable to that of enhanced alginate[27] and gelatin hydrogels.[28]

The viscoelastomeric properties of the click protein hydrogel were investigated using 5 cycles of cyclic compression test. The dissociation of non-covalent inter- and intra-molecular interactions and/or protein conformational drift cause the protein hydrogel to lose or dissipate energy upon material deformation during the loading step, resulting in reduced stress during the unloading step or a hysteresis on the loading-unloading trajectory.[29] The area of the hysteresis is used to indicate the amount energy dissipation of different hydrogels during deformation (Figure 3e). Energy dissipation is protein concentration and functional group density dependent, and ranged between 1.5 and 23 kJ/m^3. However, despite the different amount of energy dissipation for the different hydrogels, very similar amounts of energy dissipation were recorded after each successive cycles of deformation for all hydrogels (Figure 3f, g, S3c, d), indicating that these hydrogels likely undergo viscoelastic deformation during compression/deformation. These studies indicate that click hydrogels with a wide range of different mechanical properties can be prepared, pointing to their potential to be tailor-made to suit specific biomedical applications.

Next, we determined the stress-relaxation property of our click hydrogels. Tunable stress-relaxation time is desirable for promoting differentiation, cell spreading and proliferation.[30] Each protein hydrogel disk was compressed at a low strain (0.15 mm/mm) and the time needed for the stress to reduce

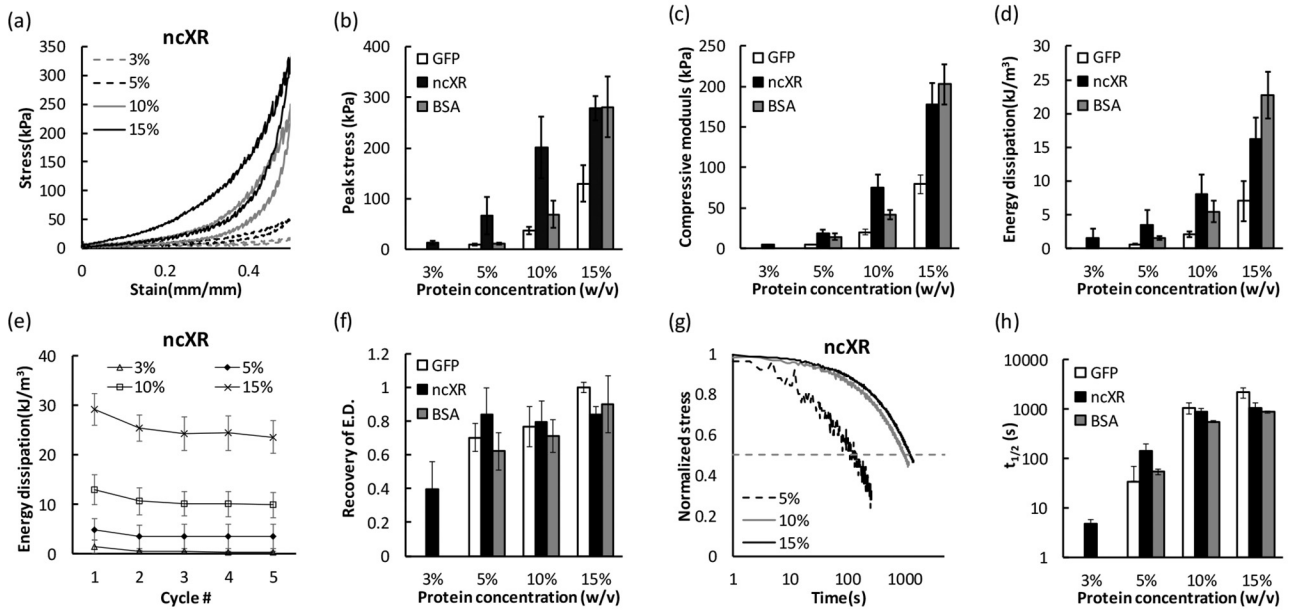

Figure 3. Mechanical characterizations of hydrogels. (a) Cyclic compression test results for ncXR hydrogel. Peak stresses at 0.5 mm/mm strain (b), compressive modulus (c) and energy dissipation amount (d) of different hydrogels. (e) The amount of energy dissipations during 5 cycles of compression for ncXR hydrogels. (f) Recovery of energy dissipation (E. D.) between the 5th and the 1st cycle cycle compared for different hydrogels. (g) Stress relaxation under 0.15 mm/mm strain for ncXR hydrogels. (h) Stress relaxation times ($t_{1/2}$) for different hydrogels.

(relax) to half of its initial value ($t_{1/2}$) was recorded (Figure 3h, i, S3e, f). All click hydrogels exhibited rapid stress-relaxation with $t_{1/2}$ range between 5 to 2200 s. The $t_{1/2}$ value increased with increasing protein concentration but did not seem to be significantly affected by the different proteins, suggesting that the stress-relaxation property is mainly influenced by inter-protein interaction rather than intra-protein interaction. The $t_{1/2}$ for click hydrogel composed of 3% and 5% w/v ncXR are 5 s and 140 s, respectively, comparable to that of alginate hydrogels.[30] At concentration above 10% w/v, the stress relaxation time appear to plateau at 1000–2000 s.

Due to the high chemical stability of N_3 and DBCO, unreacted functional groups in a protein hydrogel should remain active after gelation and thus should enable the click hydrogel to self-heal after deformation (Figure 4a). To test this hypothesis, a GFP click protein hydrogel (10% w/v, stored at 4 °C for a few weeks) was cut into two pieces with a razor blade. The two halves (A and B) were then gently pressed against each other and incubated at room temperature overnight. As a control, one of the hydrogel pieces was treated with 5 mM N_3 to block all the reactive DBCO-functional groups and then pressed against the other piece. The next day, the self-healing behavior was qualitatively assessed by picking up one half hydrogel using a pair of tweezers. If the other half hydrogel adheres to the first half hydrogel, it would confirm the ability of the hydrogel to self-heal. As shown in Figure 4b (also supplementary video 1), the two half hydrogels are strongly annealed to each other, resulting in a self-healed hydrogel disk. On the other hand, treatment with excess N_3 completely abolished the hydrogel self-healing behavior (Figure 4b, bottom), confirming that the unreacted functional groups in the hydrogel are responsible for the self-healing behavior. This hydrogel self-healing mechanism is analogous to previous polymer hydrogels employing the Schiff base,[31] host-guest interaction[32] and electrostatic interaction,[33] and is different from non-covalent hydrogels that self-heal because of their shear-thinning ability.[34]

Based on the hydrogel self-healing property, we reasoned that our click protein hydrogel should also be injectable. This injectable property is derived from the ability of small hydrogel particles to anneal to each other to form a large hydrogel. To test this hypothesis, we prepared a hydrogel in a syringe. After gelation, this hydrogel was injected into a soft tubing, which mimics the wound cavity. Under injection pressure, the click hydrogel in the syringe fractured into small pieces and passed through the needle. However, once in the soft tubing, these small pieces underwent self-healing and formed a new hydrogel contouring the shape of the tubing (Figure 4c).

Next, we evaluated the ability of click hydrogel to remember its original shape after dehydration. A hydrogel disk (10% of BSA) was air dried (Figure 4d), and then immersed in PBS at room temperature overnight. Upon rehydration, the protein film completely regained its original shape and structure after dehydration-induced deformation, indicating that both the structure of the protein and the crosslinker network are recoverable.

Since the mechanical properties of our click hydrogel fall well within the range of stresses felt by cells in nature, combined with the high biocompatibility of both protein and the click chemistry functional groups,[17] we reasoned that our click protein hydrogel should be able to support the attachment and/or encapsulation of mammalian cells. We first

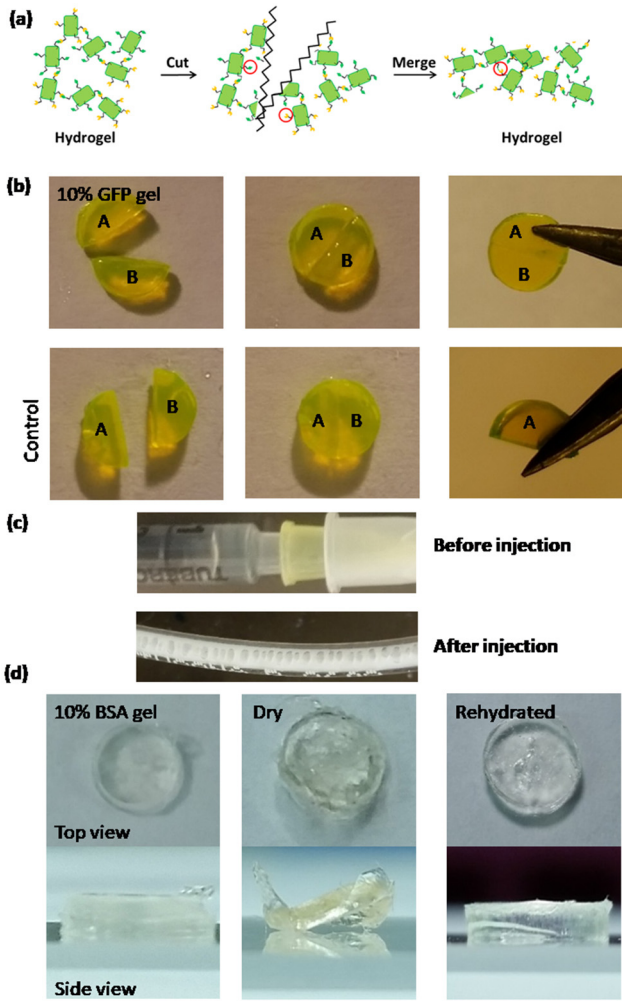

Figure 4. (a) Schematic of the self-healing mechanism of click protein hydrogels. (b) Self-healing behavior of a 10% w/v GFP hydrogel. (c) Injection of 5% w/v RGD-ncXR hydrogel. (d) A 10% w/v BSA hydrogel can regain its original shape after dehydration-induced deformation.

inserted an integrin-binding peptide – GRGDS – to one of the hydrogel building block protein to create RGD-ncXR. Hydrogel sheets (0.5 mm thickness) composed of 2.5% w/v RGD-ncXR and 2.5% w/v ncXR (in PBS) were immersed in complete growth medium for 24 h in a 6 well plate to be equilibrated before the addition of GFP^+ 293T cells (3.5×10^5 cells/cm^2). As shown in Figure 5a, the cells efficiently attached to the hydrogel sheets and adopted an elongated morphology. In addition, the cell number significantly increased between 0 (3.5×10^5 cells/cm^2), 24 (7.2×10^5 cells/cm^2) and 48 hr (20.3×10^5 cells/cm^2), indicative of rapid cell proliferation.

Next, we evaluated the ability of our click hydrogel to encapsulate mammalian cells in 3D. Functionalized hydrogel building blocks RGD-ncXR-N_3 and ncXR-DBCO (final 2.5% w/v) were first individually mixed with GFP^+ 293T cells (final 5×10^5 cells/mL), and then combined to trigger hydrogel formation, encapsulating the cells within the hydrogel network. Cells encapsulated in 3D hydrogel network adopted a rounded

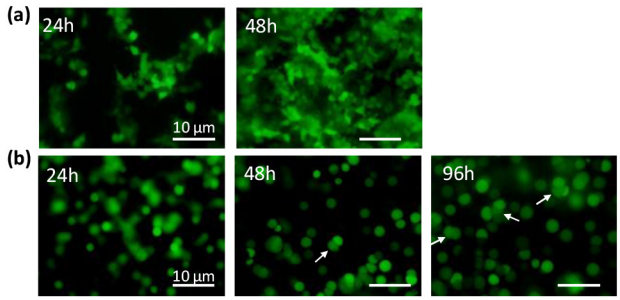

Figure 5. (a) Adhesion of GFP^+ 293T cells on a RGD-ncXR hydrogel (5% w/v) in 2D. (b) 3D cell encapsulation of GFP^+ 293T cells in RGD-ncXR hydrogels (5% w/v). Cell division was indicated by white arrows.

morphology (Figure 5b) with cell division clearly visible after 48 hr of incubation (indicated with arrows). These results demonstrated that our click protein hydrogels are highly biocompatible and are able to efficiently support mammalian cell encapsulation in 3D network.

In conclusion, we developed a new hydrogel synthesis strategy that enables any soluble proteins to be transformed into a protein hydrogel. This strategy takes advantage of the highly efficient, orthogonal and biocompatible copper-free strain-promoted azide-alkyne cycloaddition click chemistry reaction. Click protein hydrogels with a broad range of mechanical properties and stress-relaxation time can be easily produced. In addition, click protein hydrogels exhibit self-healing and shape-memory property, and are injectable, enabling the facile preparation of click hydrogels conforming to the shape of a wound cavity. Finally, the click protein hydrogels composed of integrin-binding-domain-harboring building block proteins can efficiently support mammalian cell attachment/encapsulation and facilitate robust cell proliferation, pointing to their potential to be used in a wide range of biomedical applications.

Supporting Information Summary

The Supporting Information provides the details of the experimental methods, additional figures, along with a movie demonstrating the self-healing ability of a click-protein hydrogel.

Acknowledgements

We thank the Microscope and Imaging Center at Texas A&M University for data collection. ZC and GL are partially supported by the National Science Foundation (CBET #1150478). AKG would like to acknowledge financial support from National Science Foundation (CBET 1705852), and National Institute of Health (EB026265, EB023454).

Conflict of Interest

The authors declare no conflict of interest.

Keywords: injectable · self-assemble · self-healing · shape memory · tissue engineering

[1] a) S. Banta, I. R. Wheeldon, M. Blenner, *Annu Rev Biomed Eng* **2010**; b) R. L. DiMarco, S. C. Heilshorn, *Adv Mater* **2012**, *24*, 3923–3940.
[2] a) H. D. Lu, I. R. Wheeldon, S. Banta, *Protein Eng Des Sel* **2010**, *23*, 559–566; b) W. Shen, K. Zhang, J. A. Kornfield, D. A. Tirrell, *Nature Materials* **2006**, *5*, 153–158; c) L. J. Dooling, M. E. Buck, W. B. Zhang, D. A. Tirrell, *Adv Mater* **2016**, *28*, 4651–4657.
[3] a) C. L. McGann, R. E. Akins, K. L. Kiick, *Biomacromolecules* **2016**, *17*, 128–140; b) S. Lv, D. M. Dudek, Y. Cao, M. M. Balamurali, J. Gosline, H. B. Li, *Nature* **2010**, *465*, 69–73; c) C. L. McGann, E. A. Levenson, K. L. Kiick, *Macromol Chem Physic* **2013**, *214*, 203–213.
[4] M. Larsen, V. V. Artym, J. A. Green, K. M. Yamada, *Curr Opin Cell Biol* **2006**, *18*, 463–471.
[5] E. E. Antoine, P. P. Vlachos, M. N. Rylander, *PLoS One* **2015**, *10*, e0122500.
[6] N. Yamaguchi, L. Zhang, B. S. Chae, C. S. Palla, E. M. Furst, K. L. Kiick, *J Am Chem Soc* **2007**, *129*, 3040–3041.
[7] C. T. Wong Po Foo, J. S. Lee, W. Mulyasasmita, A. Parisi-Amon, S. C. Heilshorn, *Proc Natl Acad Sci U S A* **2009**, *106*, 22067–22072.
[8] D. Guan, M. Ramirez, L. Shao, D. Jacobsen, I. Barrera, J. Lutkenhaus, Z. Chen, *Biomacromolecules* **2013**, *14*, 2909–2916.
[9] I. R. Wheeldon, J. W. Gallaway, S. C. Barton, S. Banta, *P Natl Acad Sci USA* **2008**, *105*, 15275–15280.
[10] a) M. Yamamoto, Y. Ikada, Y. Tabata, *J Biomater Sci Polym Ed* **2001**, *12*, 77–88; b) H. W. Sung, D. M. Huang, W. H. Chang, R. N. Huang, J. C. Hsu, *J Biomed Mater Res* **1999**, *46*, 520–530; c) A. Bigi, G. Cojazzi, S. Panzavolta, K. Rubini, N. Roveri, *Biomaterials* **2001**, *22*, 763–768; d) A. I. Van Den Bulcke, B. Bogdanov, N. De Rooze, E. H. Schacht, M. Cornelissen, H. Berghmans, *Biomacromolecules* **2000**, *1*, 31–38.
[11] a) F. Sun, W. B. Zhang, A. Mahdavi, F. H. Arnold, D. A. Tirrell, *Proc Natl Acad Sci U S A* **2014**, *111*, 11269–11274; b) W. B. Zhang, F. Sun, D. A. Tirrell, F. H. Arnold, *J Am Chem Soc* **2013**, *135*, 13988–13997.
[12] M. Ramirez, D. Guan, V. Ugaz, Z. Chen, *J Am Chem Soc* **2013**, *135*, 5290–5293.
[13] K. Ren, C. He, C. Xiao, G. Li, X. Chen, *Biomaterials* **2015**, *51*, 238–249.
[14] Z. Munoz, H. Shih, C. C. Lin, *Biomater. Sci.* **2014**, *2*, 1063–1072.
[15] R. Z. Lin, Y. C. Chen, R. Moreno-Luna, A. Khademhosseini, J. M. Melero-Martin, *Biomaterials* **2013**, *34*, 6785–6796.
[16] a) S. T. Koshy, R. M. Desai, P. Joly, J. Li, R. K. Bagrodia, S. A. Lewin, N. S. Joshi, D. J. Mooney, *Adv. Healthcare Mater.* **2016**, *5*, 541–547; b) V. X. Truong, M. P. Ablett, S. M. Richardson, J. A. Hoyland, A. P. Dove, *J Am Chem Soc* **2015**, *137*, 1618–1622.
[17] C. A. DeForest, B. D. Polizzotti, K. S. Anseth, *Nat Mater* **2009**, *8*, 659–664.
[18] J. Xu, T. M. Filion, F. Prifti, J. Song, *Chem.-Asian Jour.* **2011**, *6*, 2730–2737.
[19] a) C. A. DeForest, K. S. Anseth, *Angew Chem Int Ed Engl* **2012**, *51*, 1816–1819; b) A. M. Kloxin, K. J. Lewis, C. A. DeForest, G. Seedorf, M. W. Tibbitt, V. Balasubramaniam, K. S. Anseth, *Integr Biol (Camb)* **2012**, *4*, 1540–1549.
[20] J. K. Zheng, L. A. S. Callahan, J. K. Hao, K. Guo, C. Wesdemiotis, R. A. Weiss, M. L. Becker, *Acs Macro Lett* **2012**, *1*, 1071–1073.
[21] a) G. W. Ashley, J. Henise, R. Reid, D. V. Santi, *P Natl Acad Sci USA* **2013**, *110*, 2318–2323; b) A. Takahashi, Y. Suzuki, T. Suhara, K. Omichi, A. Shimizu, K. Hasegawa, N. Kokudo, S. Ohta, T. Ito, *Biomacromolecules* **2013**, *14*, 3581–3588.
[22] R. Woodyer, M. Simurdiak, W. A. van der Donk, H. Zhao, *Appl Environ Microbiol* **2005**, *71*, 1642–1647.
[23] M. C. Machczynski, E. Vijgenboom, B. Samyn, G. W. Canters, *Protein Sci.* **2004**, *13*, 2388–2397.
[24] D. Guan, Y. Kurra, W. Liu, Z. Chen, *Chem Commun (Camb)* **2015**, *51*, 2522–2525.
[25] E. A. Abou Neel, U. Cheema, J. C. Knowles, R. A. Brown, S. N. Nazhat, *Soft Matter* **2006**, *2*, 986–992.
[26] N. Annabi, S. M. Mithieux, E. A. Boughton, A. J. Ruys, A. S. Weiss, F. Dehghani, *Biomaterials* **2009**, *30*, 4550–4557.
[27] a) R. M. Desai, S. T. Koshy, S. A. Hilderbrand, D. J. Mooney, N. S. Joshi, *Biomaterials* **2015**, *50*, 30–37; b) H. Meng, P. Xiao, J. Gu, X. Wen, J. Xu, C. Zhao, J. Zhang, T. Chen, *Chem Commun (Camb)* **2014**, *50*, 12277–12280.
[28] a) S. R. Shin, S. M. Jung, M. Zalabany, K. Kim, P. Zorlutuna, S. B. Kim, M. Nikkhah, M. Khabiry, M. Azize, J. Kong, K. T. Wan, T. Palacios, M. R. Dokmeci, H. Bae, X. S. Tang, A. Khademhosseini, *ACS nano* **2013**, *7*, 2369–2380; b) J. R. Xavier, T. Thakur, P. Desai, M. K. Jaiswal, N. Sears, E. Cosgriff-Hernandez, R. Kaunas, A. K. Gaharwar, *ACS Nano* **2015**, *9*, 3109–3118.
[29] K. Ruan, G. Weber, *Biochemistry* **1989**, *28*, 2144–2153.
[30] O. Chaudhuri, L. Gu, D. Klumpers, M. Darnell, S. A. Bencherif, J. C. Weaver, N. Huebsch, H. P. Lee, E. Lippens, G. N. Duda, D. J. Mooney, *Nat Mater* **2016**, *15*, 326–334.
[31] a) F. Ding, S. Wu, S. Wang, Y. Xiong, Y. Li, B. Li, H. Deng, Y. Du, L. Xiao, X. Shi, *Soft Matter* **2015**, *11*, 3971–3976; b) T. C. Tseng, L. Tao, F. Y. Hsieh, Y. Wei, I. M. Chiu, S. H. Hsu, *Adv Mater* **2015**, *27*, 3518–3524; c) R. N. Dong, X. Zhao, B. L. Guo, P. X. Ma, *Acs Appl Mater Inter* **2016**, *8*, 17138–17150; d) S. Y. Lu, C. M. Gao, X. B. Xu, X. Bai, H. G. Duan, N. N. Gao, C. Feng, Y. Xiong, M. Z. Liu, *Acs Appl Mater Inter* **2015**, *7*, 13029–13037.
[32] K. Miyamae, M. Nakahata, Y. Takashima, A. Harada, *Angew Chem Int Ed Engl* **2015**, *54*, 8984–8987.
[33] Y. Ren, R. Y. Lou, X. C. Liu, M. Gao, H. Z. Zheng, T. Yang, H. G. Xie, W. T. Yu, X. J. Ma, *Chem Commun* **2016**, *52*, 6273–6276.
[34] a) L. Haines-Butterick, K. Rajagopal, M. Branco, D. Salick, R. Rughani, M. Pilarz, M. S. Lamm, D. J. Pochan, J. P. Schneider, *Proc Natl Acad Sci U S A* **2007**, *104*, 7791–7796; b) B. D. Olsen, J. A. Kornfield, D. A. Tirrell, *Macromolecules* **2010**, *43*, 9094–9099.

Submitted: August 25, 2017
Revised: October 25, 2017
Accepted: October 27, 2017